

RESEARCH

Open Access



Optimizing the printing parameters for dimensional accuracy of distal femur bone by using Taguchi's method

Thoudam Kheljeet Singh¹, Anil Kumar Birru^{1*}  and Khundrakpam Nimo Singh¹

*Correspondence:
birruresearch@gmail.com

¹ Department of Mechanical Engineering, National Institute of Technology Manipur, Langol, Imphal, Manipur 795004, India

Abstract

Background: Fused deposition modelling (FDM) is a popular additive manufacturing technique with capability of producing complex and integrate shapes. One of the critical aspects of FDM is the dimensional accuracy of 3D (three-dimension) printed model, especially in medical science applications, as proper fit and function with human body can prevent patient's discomfort, complication or even harm.

Objective: In this research work, the optimisation of print parameters: layer height, nozzle temperature, printing speed, infill pattern and infill density for improving the dimensional accuracy of distal femur bone, an irregular and complex shaped geometry is carried out using Taguchi's method and to study its influence using ANOVA (analysis of variance).

Methodology: 3D CAD (computer-aided design) model of the distal femur bone is generated from a CT (computerized tomography) scan using 3D slicer and its associated errors are corrected using Ansys SpaceClaim. The model is prepared for printing using Ultimaker Cura as per L_{16} orthogonal array experimental layout where TEA (trans epicondylar axis), which is the distance between the most prominent point of the lateral and medial epicondyle, is set at 45° from X-axis in XY plane, i.e. diagonally on the plane of printing bed. It is then printed with PLA (polylactic acid) filament. Length along TEA is compared accordingly with 3D CAD model. Taguchi's method of 'smaller the better' is applied for reducing deviation. Further, ANOVA analysis is done on the data set and a linear regression model is also developed.

Result: Through Taguchi's method, the optimum parameters were found to be triangle for infill pattern, 200 °C for nozzle temperature, 30 mm/s for nozzle speed, 0.1 mm for layer height and 40% for infill density. ANOVA analysis shows that all parameters contribute significantly with layer height being the most influential parameter, followed by infill pattern, nozzle speed, nozzle temperature and infill density. Mathematical model through multiple linear regression method was developed with determination of coefficient value of 96.91% and standard residual value is within the acceptable range of ± 2 indicating that there is no outlier in the data.

Keywords: Fused deposition modelling, Dimensional accuracy, Distal femur bone, Parameters optimisation, PLA

Introduction

FDM (fused deposition modelling) is a widely used additive manufacturing technique that has the capability of producing complex and integrated shapes [1]. Its applicability can be found in various fields such as medicine, industry, agriculture, etc. [2–4]. It works by melting thermoplastic filament and extruding it layer by layer through the nozzle to create the model as per 3D CAD (computer-aided drawing) model data [5, 6]. One of the critical aspects of FDM is the dimensional accuracy of the printed model especially in medical science applications [7, 8]. The dimensional accuracy of a model in general is to ensure proper fit and assembly, to maintain quality functional prototypes or products, especially in the field of medical science as FDM is used to create custom implants, prosthetics and anatomical models for surgical guides. A 3D print of custom anatomical model for implants or a surgical guide with accurate dimensions will ensure the safety of patient as a proper fit and function with the human body will avoid the patient's discomfort, complication or even harm [9–11]. Our proposed research focuses on the dimensional accuracy of custom 3D printed distal femur as knee replacement surgery is a frequently performed procedure worldwide, with hundreds of thousands of surgeries conducted annually [12]. With the help of the printed model of distal femur bone, customised femoral component of the knee implant can be manufactured which will be beneficial compared to the standard implants currently available in the markets by reducing the reduction of healthy bone. The printed model can also act as a surgical guide for complicated surgery [11]. With the increase in the research of bioactive composite that can be 3D printed such as PLA—hydroxyapatite composite, PLA—chitosan composite, etc. [13] for the printing of customised implants, our research work might be used as a basis for printing with greater dimensional accuracy.

The dimensional deviation of the 3D printed model is affected by various factors such as shrinkage or warping, stepping effect, overhanging structure without support at a higher angle, build direction, etc. which are influenced by various 3D printing parameters [14–18]. These parameters have been studied by various researchers to reduce the dimensional deviation of the 3D printed model.

Agarwal et al. [19] examined the print parameters' effect including print speed, wall thickness, infill density, layer thickness, build plate temperature and extrusion temperature on the dimensional accuracy of central composite design 3D printed model using ABS. Robles et al. [20] analysed the effect of layer thickness and infill density of FDM on dimensional accuracy of ABS parts by printing cubic shapes. Bolat et al. [21] analysed the layer height's effect on the dimensional accuracy of PLA, PET-G and ABS on 3D printed model of standard ASTM D638-14 type IV. Suaidi et al. [22] optimized the FDM printing parameters viz. layer thickness, infill density and build orientation for improving the surface roughness, dimensional accuracy and tensile strength using 3D printed ASTM D638-14 type IV model. Mohanty et al. [23] examined the effect of raster angle, part orientation, air gap, layer thickness and raster width on the dimensional accuracy of a 3D-printed geometrical model using ABS material. Akbas et al. [24] examined the influence of nozzle temperature and feed rates on the dimensional accuracy of PLA

and ABS using strip as printed models. Zharylkassyn et al. [25] reviewed over 31 articles that examined the effect of layer thickness, part orientation and extrusion temperature in terms of the material used viz. ABS, PLA, etc. on the dimensional accurateness of printed model.

Various parameters and their significances concerning the dimensional accurateness of the printed model have been extensively examined through the use of standard geometrical 3D models such as cylinder, cuboid, ASTM D638-14 type IV model, etc., yet, no researchers have attempted to study an irregular and complex shape geometry such as human anatomy. Hence, our research focuses on improving the dimensional accuracy of 3D printed model of distal femur bone through the optimisation of five significant FDM printing parameters viz. layer height, nozzle temperature, infill density, printing speed and infill pattern with four levels each using Taguchi's method. Furthermore, the significance and its effect on dimensional accuracy are analysed using ANOVA. A linear regression model, using the experimental data, is developed to understand the correlation between the dimensional deviation and printing parameters. The linear regression model is validated by comparing it with the experimental data. Overall, this research will help in the fabrication of dimensionally accurate customised implants, implant mould and other complex and irregularly shaped geometry.

Methods

This research aims to optimize the FDM print parameters for dimensional accuracy of an irregular and complex shape using distal femur bone through Taguchi's method. A flowchart of the process employed for the research is shown in Fig. 1. The CT scan of a patient is imported into the 3D slicer software where 3D CAD model is exported in STL file format from DICOM file format. The errors associated with the STL file 3D model are corrected with the help of Ansys SpaceClaim. Once the correction is done to the STL file model, the model is then imported into the Ultimaker Cura, the model across which the length is to be measured i.e., trans epicondylar axis (TEA), which is the distance between the most prominent point of the lateral and medial epicondyle, is set at 45° from X-axis in XY plane i.e. diagonally on the plane of printing bed as shown in Fig. 2.

Polylactic acid (PLA) filament is considered as the printing material. PLA is one of the most commonly used materials because of its low cost, easily available, comparatively low toxicity and low print temperature [26, 27]. PLA is also a biocompatible material which researchers have been using PLA as base material for making bioactive composite material [13]. The low thermal coefficient of PLA highly influences dimensional accuracy as it influences the expansion and shrinkage [28]. Similarly, good intra-bonding of layers of PLA helps in maintaining the dimension of the model. The colour of the PLA filament and the fabrication process of PLA was also observed to be influencing the dimensional accuracy which is due to colour dependent on process crystallinity or difference in thermal properties due to the presence of colour additives [29–31].

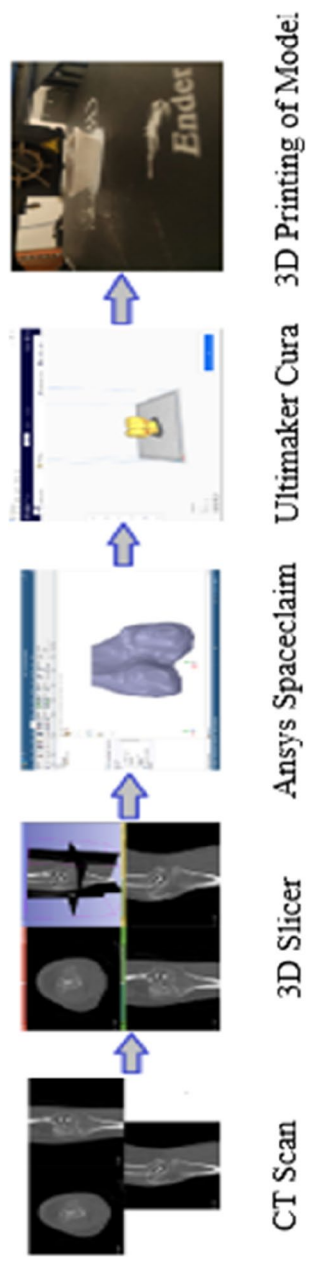


Fig. 1 Flowchart of the process employed in this study from CT scan to printed 3D model

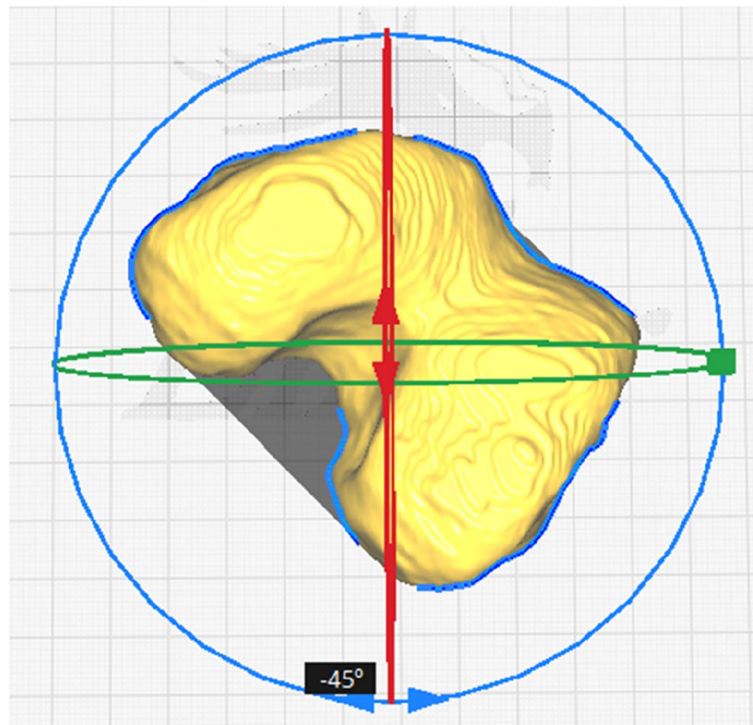


Fig. 2 TEA of distal femur bone set at 45° angle from X-axis in Ultimaker Cura

A pilot test was conducted to determine the range of FDM printing parameters that affect the dimensional accuracy of the 3D-printed models. Accordingly, the printing parameters and their range that have been considered are infill pattern which is made to vary between lines, cubic, triangle and octet, infill density is varied between 20 to 80% with a step size of 20%, layer height is varied from 0.1 mm to 0.4 mm with a step size of

Table 1 Control FDM printing parameters with 4 levels each

Parameter	Level 1	Level 2	Level 3	Level 4
Infill pattern	Lines	Triangles	Cubic	Octet
Nozzle temperature (°C)	200	205	210	215
Printing speed (mm/s)	30	70	110	150
Layer height (mm)	0.1	0.2	0.3	0.4
Infill density (%)	20	40	60	80

Table 2 Fixed FDM printing parameters

Parameters	Value
Bed temperature	50 °C
Build plate adhesive type	Brim
Line width	0.4 mm
Wall thickness	0.8 mm
Wall line count	2
Fan speed	100%
Infill layer thickness	0.1 mm
Infill overlap percentage	30%

0.1 mm, nozzle temperature is varied from 200 °C to 215 °C with a step size of 5 °C and print speed is varied from 30 mm/s to 150 mm/s with a step size of 40 mm/s shown in Table 1. The parameters shown in Table 2 are fixed while the remaining parameters are set as per the default setting of the Ultimaker Cura. The experimental layout if used in full factorial design, the total experiment to be conducted will be 1024, i.e. 4^5 for 5 factors and 4 levels; however, through the use of Taguchi's method of orthogonal array, the total number of experiments can be reduced while giving statically same valid result. As the degree of freedom (DOF) in Taguchi's design is given by subtracting 1 from number of levels, the DOF for each factor with 4 level will be 3. Therefore, the total DOF for 5 factors with 4 level will be 15. The appropriate orthogonal array will be L_{16} . Hence, an experimental layout of the print parameters as per L_{16} orthogonal array is listed in Table 3. Additionally, to observe the improvement in accurateness of dimension, a model is prepared for printing as a baseline model with the default setting of ultimaker cura where infill pattern is cubic shaped, layer height is 0.2 mm, infill density of 20%, nozzle temperature of 200 °C and with a print speed of 50 mm/s. All these parameters are then set accordingly and slicing is done. The G code is then transferred to the FDM printer (Creality Ender 3 Pro) and models are then printed accordingly using PLA filament of 1.75 mm diameter as printing material. A digital vernier calliper with a least count of 0.01 mm is used for measuring the 3D printed distal femur bone across the trans epicondylar axis (TEA). The measurement is taken thrice to reduce human errors in the measurement. The measurement is then compared with the TEA length measured in 3D CAD model using Ansys SpaceClaim and absolute deviation is calculated using Eq. 1.

$$\text{Absolute Deviation} = |\text{TEA length of 3D printed model} - \text{TEA length of 3D CAD model}| \quad (1)$$

Table 3 Experimental layout of the print parameters using L_{16} orthogonal array

Experiment no	Infill pattern	Nozzle temperature (°C)	Print speed (mm/sec)	Layer height (mm)	Infill density (%)
1	Lines	200	30	0.1	20
2	Lines	205	70	0.2	40
3	Lines	210	110	0.3	60
4	Lines	215	150	0.4	80
5	Triangles	200	70	0.3	80
6	Triangles	205	30	0.4	60
7	Triangles	210	150	0.1	40
8	Triangles	215	110	0.2	20
9	Cubic	200	110	0.4	40
10	Cubic	205	150	0.3	20
11	Cubic	210	30	0.2	80
12	Cubic	215	70	0.1	60
13	Octet	200	150	0.2	60
14	Octet	205	110	0.1	80
15	Octet	210	70	0.4	20
16	Octet	215	30	0.3	40

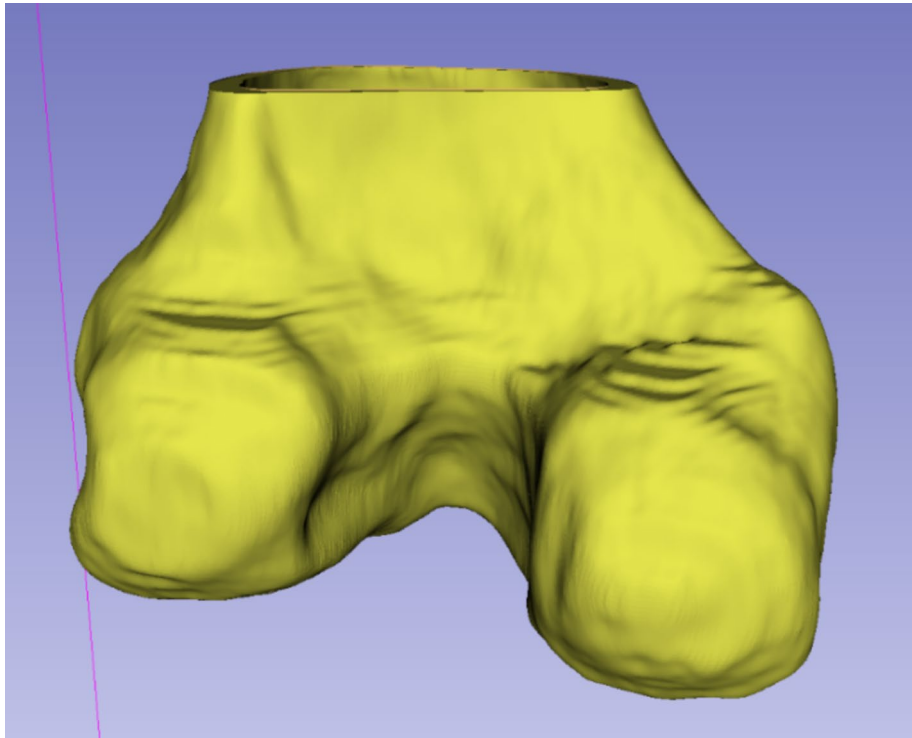


Fig. 3 3D CAD model of distal femur bone in STL file format generated from CT scan using 3D slicer software

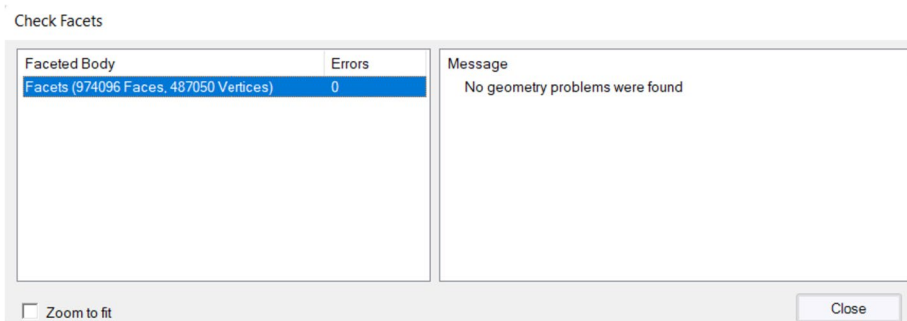


Fig. 4 Ensuring error-free STL 3D model using Ansys SpaceClaim software

Results and discussion

Modelling and printing of distal femur bone

3D model of the distal femur bone as shown in Fig. 3 is generated from CT scan to STL file format using 3D slicer. The final model generated from Ansys SpaceClaim after the correction of STL file format has about 974,096 faces and 487,050 vertices as shown in Fig. 4. The model is then sliced into individual layers and converted the STL file into G code using Ultimaker Cura. The G code makes the tools in the 3D printer move as per the generated layer information during the slicing process. A total of 16 models are printed accordingly as shown in Fig. 5.



Fig. 5 3D printed distal femur bone as per the experimental layout of L_{16} orthogonal array

Table 4 Absolute dimensional deviation of TEA of 3D printed distal femur bone with S/N ratio and mean

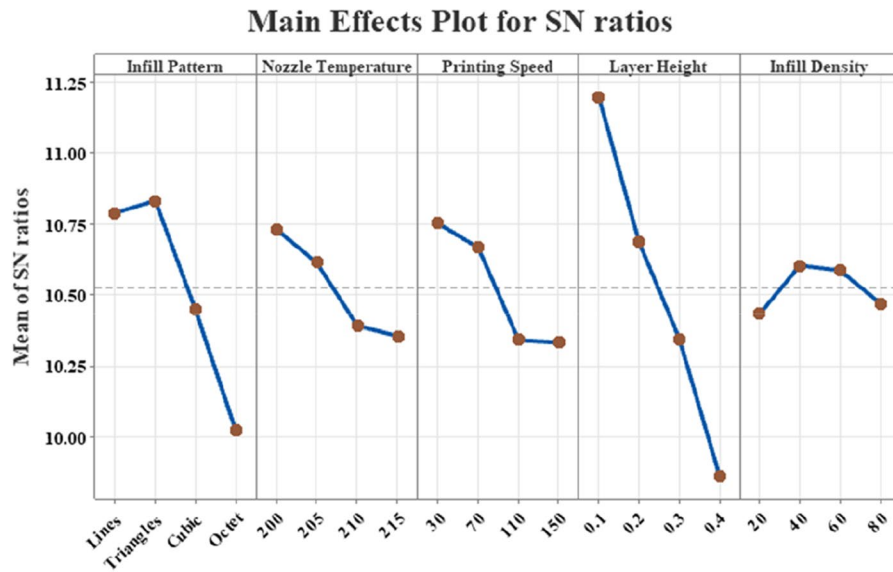
Experiment no	Deviation 1	Deviation 2	Deviation 3	Mean	SN ratio
1	0.25	0.26	0.26	0.256667	11.8111
2	0.28	0.27	0.27	0.273333	11.2649
3	0.30	0.31	0.30	0.303333	10.3605
4	0.32	0.33	0.33	0.326667	09.7170
5	0.29	0.28	0.28	0.283333	10.9528
6	0.30	0.29	0.30	0.296667	10.5535
7	0.27	0.27	0.28	0.273333	11.2649
8	0.29	0.30	0.30	0.296667	10.5535
9	0.33	0.31	0.32	0.320000	09.8942
10	0.31	0.32	0.31	0.313333	10.0789
11	0.29	0.30	0.29	0.293333	10.6517
12	0.28	0.28	0.27	0.276667	11.1596
13	0.31	0.31	0.30	0.306667	10.2656
14	0.29	0.30	0.30	0.296667	11.5535
15	0.34	0.34	0.35	0.343333	09.2849
16	0.31	0.32	0.32	0.316667	09.9870

Optimisation of the printing parameters for dimensional accuracy

The length of TEA in 3D CAD model, when measured using Ansys SpaceClaim, is 79.72 mm. The absolute deviation of the printed model from that of the 3D CAD model is calculated using Eq. 1 and is listed in Table 4. The model printed as baseline was found to deviate with an absolute mean value of 0.2933 mm. As lower deviation of the model is required to increase the dimensional accuracy of the model, Taguchi's

Table 5 Signal-to-noise ratio for each level of each parameter along with delta value

Level	Infill pattern	Nozzle temperature	Printing speed	Layer height	Infill density
1	10.788	10.731	10.751	11.197	10.432
2	10.831	10.613	10.666	10.684	10.603
3	10.446	10.390	10.340	10.345	10.585
4	10.023	10.354	10.332	9.862	10.469
Delta	0.808	0.377	0.419	1.335	0.171
Rank	2	4	3	1	5



Signal-to-noise: Smaller is better

Fig. 6 Signal-to-noise ratios graph for each parameter using smaller is better characteristic

‘smaller the better’ characteristic is taken into consideration whose value is given by the formula:

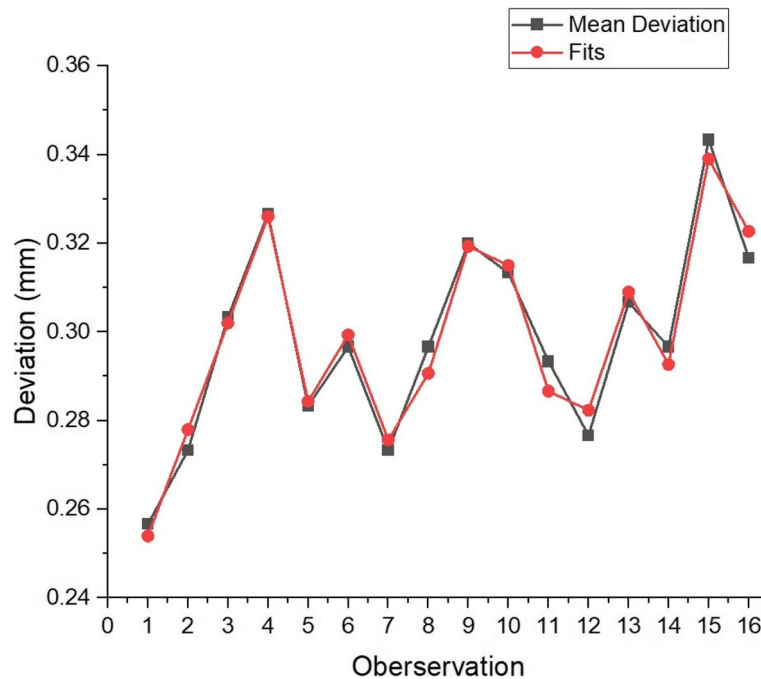
$$\text{Signal to Noise} \left(\frac{S}{N} \right) = -10 \left(\log \left(\frac{\sum Y^2}{n} \right) \right) \tag{2}$$

where ‘Y’ is the result value, i.e. absolute deviation and ‘n’ is the number of experiments.

The absolute deviation along with the value for signal-to-noise ratio (S/N) calculated using Eq. 2 is listed in Table 4. The S/N ratio for each level base on the smaller is better characteristic is shown in Table 5 which identifies the optimum parameter, i.e. parameter with the highest S/N ratio for lowering of absolute deviation and the influence of each factor has been ranked accordingly as per the Delta value. Therefore, as per the mentioned values in Table 5 and the graph shown in Fig. 6, the optimal parameter for higher dimensional accuracy is when the infill pattern is triangular, nozzle temperature is 200 °C, printing speed is 30 mm/s, layer height is 0.1 mm and infill density is 40%.

Table 6 ANOVA analysis of the result

Source	DF	Seq SS	Contribution	Adj SS	Adj MS	F-value	P-value
Infill pattern	3	0.005990	24.75%	0.005990	0.001997	53.24	0.000000
Nozzle temperature	3	0.001373	5.67%	0.001373	0.000458	12.20	0.000017
Printing speed	3	0.001823	7.53%	0.001823	0.000608	16.20	0.000001
Layer height	3	0.013423	55.47%	0.013423	0.004474	119.31	0.000000
Infill density	3	0.000390	1.61%	0.000390	0.000130	3.46	0.027583
Error	32	0.001200	4.96%	0.001200	0.000038		
Total	47	0.024198	100.00%				

**Fig. 7** Comparative graph between the measured absolute deviation and fits

The data is further analysed using ANOVA whose result is shown in Table 6. It can be seen that all values of p are very close to 0; hence, the null hypothesis can be rejected. This indicates that all the printing parameters are of very significant in relation to the dimension accuracy of the 3D printed model. The layer height has the highest contribution of 55.47% in regards to improvement in the dimensional accuracy, followed by an infill pattern of 24.75%, then by printing speed, nozzle temperature and infill density. The infill density has the least contribution in regards to dimensional accuracy. Further, the linear regression analysis is performed on the data set which generates an empirical equation for a predictive mathematical model as shown below in Eq. 3 with determination of coefficient, R^2 value of 96.91%. The empirical equation, i.e. linear regression model helps in establishing a relation between the dependent variable, i.e. absolute deviation and independent variables which are the 3D printing parameters.

Table 7 A comparative table between mean absolute deviation and fits calculated using linear regression model

Observation	Mean	Fits	Residual	Standardized residual
1	0.256667	0.254	0.002667	0.895127
2	0.273333	0.278	-0.00467	-1.0255
3	0.303333	0.302	0.001333	0.292999
4	0.326667	0.326	0.000667	0.223782
5	0.283333	0.284333	-0.001	-0.26001
6	0.296667	0.299333	-0.00267	-0.69336
7	0.273333	0.275667	-0.00233	-0.60669
8	0.296667	0.290667	0.006	1.560065
9	0.320000	0.319333	0.000667	0.173341
10	0.313333	0.315	-0.00167	-0.43335
11	0.293333	0.286667	0.006667	1.733406
12	0.276667	0.282333	-0.00567	-1.47339
13	0.306667	0.309	-0.00233	-0.60669
14	0.296667	0.292667	0.004	1.040043
15	0.343333	0.339	0.004333	1.126714
16	0.316667	0.322667	-0.006	-1.56007

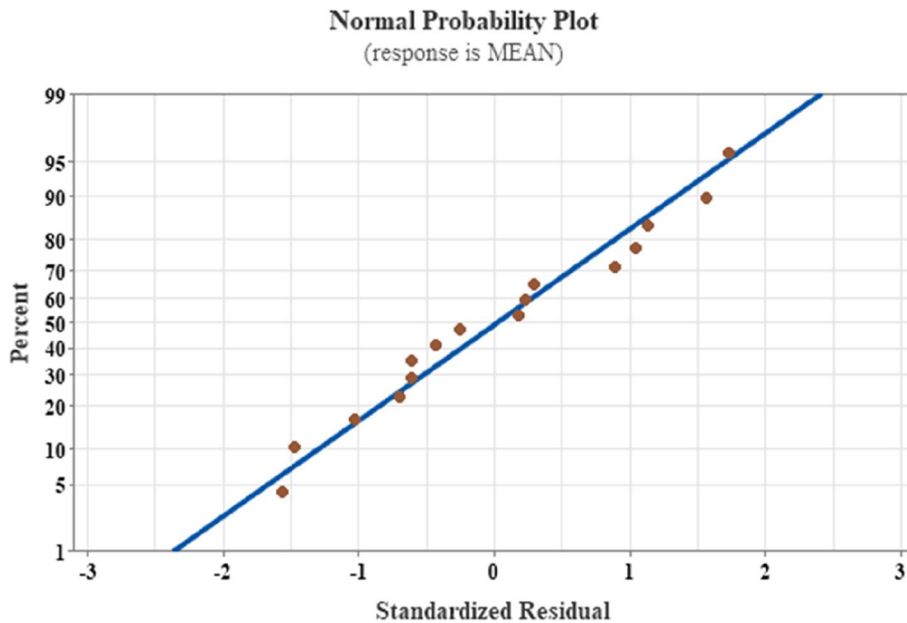


Fig. 8 Normal probability graph plot for standardized residual

To validate the empirical equation, a comparison is made between the absolute mean deviation and calculated deviation (fits) as shown in a graph in Fig. 7 and Table 7 which shows that both are in agreement with a little difference between them. The normal probability graph shown in Fig. 8 shows that the standard residual value is within the acceptable range of ± 2 indicating that there is no outlier in the data.

Infill pattern

$$\begin{aligned}
 \text{Cubic MEAN Deviation} &= .0634 + 0.000917 \text{ Nozzle Temperature} + 0.000131 \text{ Printing Speed} \\
 &\quad + 0.1492 \text{ Layer Height} - 0.000038 \text{ Infill Density} \\
 \text{Lines MEAN Deviation} &= 0.0526 + 0.000917 \text{ Nozzle Temperature} + 0.000131 \text{ Printing Speed} \\
 &\quad + 0.1492 \text{ Layer Height} - 0.000038 \text{ Infill Density} \\
 \text{Octet MEAN Deviation} &= 0.0784 + 0.000917 \text{ Nozzle Temperature} \\
 &\quad + 0.000131 \text{ Printing Speed} + 0.1492 \text{ Layer Height} - 0.000038 \text{ Infill Density} \\
 \text{Triangles MEAN Deviation} &= 0.0501 + 0.000917 \text{ Nozzle Temperature} + 0.000131 \text{ Printing Speed} \\
 &\quad + 0.1492 \text{ Layer Height} - 0.000038 \text{ Infill Density}
 \end{aligned} \tag{3}$$

Validation of the result

Layer height highly influences the dimension accuracy of the 3D printed distal femur bone as seen from ANOVA analysis in Table 6. The optimal dimension is achieved when the layer height is 0.1 mm. With an increase in the layer height, it is observed that the dimensional deviation increased as seen in the S/N graph shown in Fig. 6 as PLA is deposited from the nozzle in the molten state; due to its fluidity, it bulges out which results in dimensional deviation. The increase in layer height increases the volume of the material which in turn increases the bulging of material resulting in greater dimensional deviation. The dimensional deviation is further amplified by the staircase effect [32]. This makes the layer height the most significant parameter among the other parameters in controlling dimensional accuracy. The result observed in this research is similar to the finding of Nidagundi et al. [33] and Polak et al. [26].

Among the four infill pattern types, the optimal infill pattern is observed with triangle infill pattern which is similar to the finding of Alafaghani et al. [34] where the dimensional accuracy is observed with diamond infill pattern. The diamond infill pattern is similar to the triangular infill as combining the base of two triangles forms the diamond infill. The dimensional accuracy decreases with linear infill pattern followed by cubic infill pattern. The highest dimensional deviation is observed with octet infill pattern.

The dimensional deviation of the distal femur bone increases as the printing speed increases from 30 mm/s to 150 mm/s as the time available for proper deposition of the material decreases. Hence, the optimal printing speed for dimensional accuracy is observed at 30 mm/s. It is in sync with the findings of Polak et al. [26] and Alafaghani et al. [34].

Optimal nozzle temperature for dimensional accuracy of the printed distal femur bone is observed at 200 °C. The dimensional deviation increases as the nozzle temperature increases from 200 °C to 215 °C. This is due to an increase in the fluidity of PLA with increasing temperature thereby making the dimensional control difficult as PLA expands freely [34–36]. The observation made in this research is in line with the findings of Akbas et al. [24], Kaveh et al. [37] and Frunzaverde et al. [27].

Even though infill density is significant concerning dimensional accuracy, its contribution among the other control print parameters is less. The optimal infill density for dimensional accuracy of the printed distal femur bone is observed at 40%. The accuracy increases as the infill density increases from 20 to 40% but the dimensional deviation

increases as the density increases from 40 to 80% with a slight variation of dimensional difference between the printed distal femur bone with 40% and 60%. This observation is similar to the finding of Alafaghani et al. [34] and Suaidi et al. [22]. The increase in accuracy with an increase in infill density is due to the presence of high volume of molten material and lesser space within the printed model part causing it to flow outwards which counteract the dimensional error due to the shrinkage [18]. However, with further increase in the infill density, dimensional error increases as internal stress is created within the part due to uneven heat distribution during cooling and solidification with increases in density as the shrinkage cycle of the molten material increases resulting in warping and distortion making it difficult to maintain or control dimensional accuracy [19].

The observations made in this research are validated as it is in line with the finding of various researchers.

Optimal 3D printing parameter

The obtained optimum 3D printing parameter using Taguchi's method of smaller the better characteristic as shown in Table 8 is used for printing the model. The TEA of 3D printed distal femur bone is measured using a digital vernier calliper. Its absolute mean deviation is also compared with that of the deviation calculated (fits) using the empirical equation in the Eq. 3 as shown in Table 9. The value obtained is within the 95% confidence interval of between 0.241035 and 0.260465. Overall, it can be seen that the obtained absolute mean deviation with the optimum printing parameters is less than the other deviation. The printed model using the optimum parameter is shown in Fig. 9.

Overall evaluation of process parameters

Figure 10 shows a graph that compares the dimensional accuracy of 16 sets of printed models with that of model printed with optimum parameters and baseline model. When compared to the baseline model that is printed with the default setting of Ultimaker Cura with that of the optimum parameters, dimensional accuracy is improved by 17.24%, i.e. by 0.05 mm. The difference between them is less as the layer height of baseline model is 0.1 mm more than that of the optimum, the difference in speed is 20 mm/s and the density of the baseline model is less by 20% while the temperature is same in both cases. As layer height and infill pattern contribute significantly more than others, the dimensional difference in between the baseline and optimum model did not differ significantly. This can be seen from Table 10 that in model 1, when the infill pattern and layer height are maintained same with that of the optimum parameters, the mean dimensional deviation is of 0.25667 which is closer to the dimension deviation of the optimum model whereas in model 2, when the infill pattern and layer height is maintained same with that of the baseline parameters, the mean dimensional deviation is of 0.27333 which is closer to the dimension deviation of the baseline model. The difference in the dimensional deviation of model 1 and 2 also iterates the significant contribution of layer height and infill pattern. The 3D printed distal femur bone of baseline, model 1 and model 2 is shown in Fig. 11.

Table 8 Optimum 3D printing parameter with respect to dimensional accuracy

Infill pattern	Nozzle temperature	Printing speed	Layer height	Infill density
Triangle	200°C	30 mm/s	0.1 mm	40%

Table 9 Dimensional deviation of the 3D printed model using optimal value

Deviation 1	Deviation 2	Deviation 3	Mean	Fits	Residual
0.24	0.25	0.24	0.24333	0.25075	-0.00742

**Fig. 9** 3D printed model of the distal femur bone using optimum parameter

The limitation of our research is the unable to control the environmental factors such as ambient temperature, humidity, etc. which can affect the material, printing process and, consequently, dimensional accurateness of the model [35].

Conclusions

This research paper focuses on the optimisation of the important printing parameters viz. infill pattern, nozzle temperature, printing speed, layer height and infill density for improvement in dimensional accuracy of the irregular and complex shape of human anatomy (distal femur bone) when measured along the TEA which was aligned at a 45°

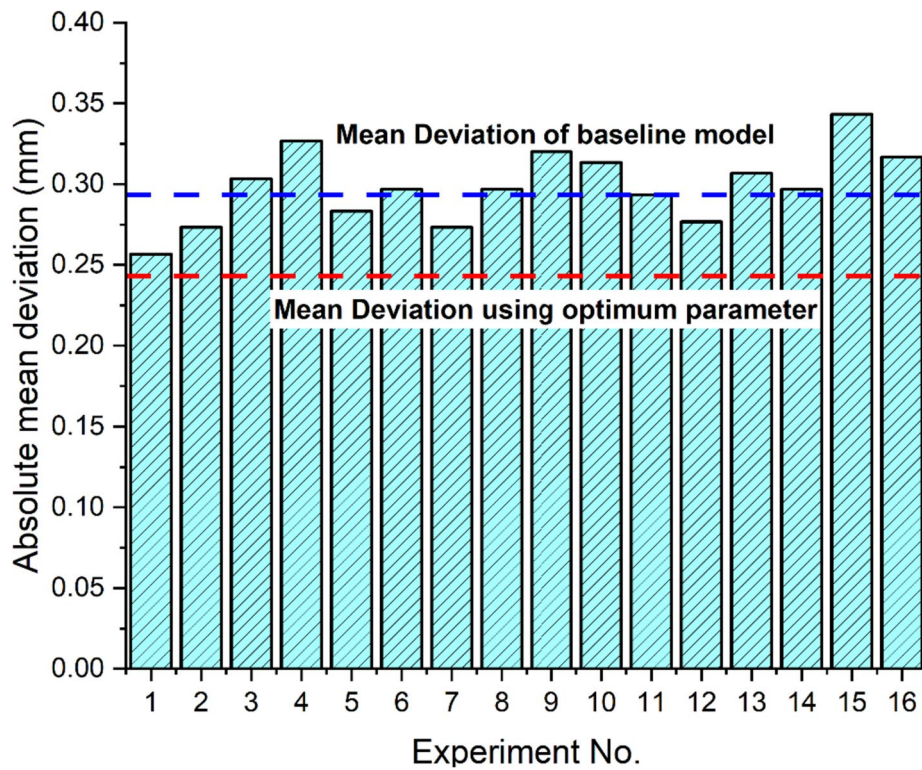


Fig. 10 Comparative graph of absolute mean deviation of the 3D printed model of distal femur

angle from X -axis in XY plane. The printing of the distal femur bone was done as per the L_{16} orthogonal array experimental layout of the 3D printing parameter. Following are the results that have been observed:

- Using the 'smaller the better' characteristic of Taguchi's method, the minimum dimensional deviation was observed when infill pattern is Triangle; nozzle temperature is at 200 °C; nozzle speed is 30 mm/s; layer height is 0.1 mm; and infill density is of 40%.
- ANOVA analysis of the data has shown that all the parameters contribute significantly as the p -value is very close to 0. The dimensional accuracy of the distal femur bone was highly influenced by layer height with a contribution of 55.47% followed infill pattern of 24.75%, then by printing speed, nozzle temperature and infill density.
- A close agreement was observed between the fits and the experimental absolute deviation in the developed linear regression model. This empirical equation can be used for the prediction of absolute deviation for the given printing parameters.

Table 10 3D printing parameters for models 1 and 2

Model	Infill pattern	Nozzle temperature (°C)	Print speed (mm/s)	Layer height (mm)	Infill density (%)	Absolute mean deviation (mm)
1	Triangle	200	50	0.1	20	0.25667
2	Cubic	200	30	0.2	40	0.27333



Fig. 11 3D printed distal femur bone of baseline, model 1 and model 2

The present research work emphasised only on the optimization of dimensional accurateness of the model. Further studies could investigate the optimum printing parameters of FDM with multiple objectives of improving the strength and shortening the time required for printing while maintaining the dimensional accuracy of the model. This proposed research work might help in producing material of good strength and dimensionally accurate models with shorter print time.

Abbreviations

3D	Three dimension
ABS	Acrylonitrile butadiene styrene
ANOVA	Analysis of variance
ASTM	American Society for Testing and Materials
CAD	Computerized-aided design
CT	Computerized tomography
DICOM	Digital Imaging and Communication in Medicine
FDM	Fused deposition modelling
PET-G	Polyethylene terephthalate glycol
PLA	Polylactic acid
S/N ratio	Signal to noise ratio
STL	STereoLithography
TEA	Trans epicondylar axis

Acknowledgements

The first author (Enrolment no. 22407005) would like to thank the National Institute of Technology, Manipur, for their support in carrying out the research. We are also grateful to Akumen AI Pvt. Ltd. for allowing us to use its facility.

Authors' contributions

TKS performed the experimentation and analysis of the result and drafted the manuscript. AKB and KNS supervised the work, reviewed and edited the manuscript. All authors read and approved the final manuscript.

Funding

No funding was received for conducting this study.

Availability of data and materials

The datasets used and analysed during the current study are available from the corresponding author on reasonable request.

Declarations

Competing interests

The authors declare that they have no competing interests.

Received: 20 June 2023 Accepted: 8 December 2023

Published online: 03 January 2024

References

1. Turner BA, Strong R, Gold SE (2014) A review of melt extrusion additive manufacturing processes: I. Process design and modeling. *Rapid Prototyp J* 20(3):192–204.
2. Pearce JM (2015) Applications of open source 3-D printing on small farms. *Org Farming* 1(1). <https://doi.org/10.12924/of2015.01010019>
3. Zuniga J, Katsavelis D, Peck J, Stollberg J, Petrykowski M, Carson A, Fernandez C (2015) Cyborg beast: a low-cost 3D-printed prosthetic hand for children with upper-limb differences. *BMC Res Notes* 8(1):10. <https://doi.org/10.1186/s13104-015-0971-9>
4. Bikas H, Stavropoulos P, Chryssolouris G (2015) Additive manufacturing methods and modeling approaches: a critical review. *Int J Adv Manuf Technol* 83(1–4):389–405. <https://doi.org/10.1007/s00170-015-7576-2>
5. Kun K (2016) Reconstruction and development of a 3D printer using FDM technology. *Procedia Eng* 149:203–211. <https://doi.org/10.1016/j.proeng.2016.06.657>
6. Gardan J (2015) Additive manufacturing technologies: state of the art and trends. *Int J Prod Res* 54(10):3118–3132. <https://doi.org/10.1080/00207543.2015.1115909>
7. Equbal A, Equbal MdA, Sood AK, Pranav R, Equbal Mdl (2018) A review and reflection on part quality improvement of fused deposition modelled parts. *IOP Confer Ser Mater Sci Eng* 455:012072. <https://doi.org/10.1088/1757-899x/455/1/012072>
8. Gendviliene I, Simoliunas E, Rekstyte S, Malinauskas M, Zaleckas L, Jegelevicius D, Bukelskiene V, Rutkunas V (2020) Assessment of the morphology and dimensional accuracy of 3D printed PLA and PLA/HAP scaffolds. *J Mech Behav Biomed Mater* 104:103616. <https://doi.org/10.1016/j.jmbbm.2020.103616>
9. George E, Liacouras P, Rybicki FJ, Mitsouras D (2017) Measuring and establishing the accuracy and reproducibility of 3D printed medical models. *Radiographics* 37(5):1424–1450. <https://doi.org/10.1148/rg.2017160165>
10. Bozkurt Y, Karayel E (2021) 3D printing technology; methods, biomedical applications, future opportunities and trends. *J Market Res* 14:1430–1450. <https://doi.org/10.1016/j.jmrt.2021.07.050>
11. Meyer-Szary J, Luis MS, Mikulski S, Patel A, Schulz F, Tretiakow D, Fercho J, Jaguszewska K, Frankiewicz M, Pawłowska E, Targoński R, Szapak Ł, Dądela K, Sabiniewicz R, Kwiatkowska J (2022) The role of 3D printing in planning complex medical procedures and training of medical professionals—cross-sectional multispecialty review. *Int J Environ Res Public Health* 19(6):3331. <https://doi.org/10.3390/ijerph19063331>
12. Price AJ, Alvand A, Troelsen A, Katz JN, Hooper G, Gray A, Carr A, Beard D (2018) Knee replacement. *Lancet* 392(10158):1672–1682. [https://doi.org/10.1016/S0140-6736\(18\)32344-4](https://doi.org/10.1016/S0140-6736(18)32344-4)
13. Bernardo MP, da Silva BCR, Hamouda AEI, de Toledo MAS, Schalla C, Rütten S, Goetzke R, Mattoso LHC, Zenke M, Sechi A (2022) PLA/hydroxyapatite scaffolds exhibit in vitro immunological inertness and promote robust osteogenic differentiation of human mesenchymal stem cells without osteogenic stimuli. *Sci Rep* 12:2333. <https://doi.org/10.1038/s41598-022-05207-w>
14. Armillotta A, Bellotti M, Cavallaro M (2018) Warpage of FDM parts: experimental tests and analytic model. *Robot Comput Integr Manuf* 50:140–152. <https://doi.org/10.1016/j.rcim.2017.09.007>
15. Abeykoon C, Sri-Amphorn P, Fernando A (2020) Optimization of fused deposition modeling parameters for improved PLA and ABS 3D printed structures. *Int J Lightweight Mater Manuf* 3(3):284–297. <https://doi.org/10.1016/j.ijlmm.2020.03.003>
16. Mohamed OA, Masood SH, Bhowmik JL (2021) Modeling, analysis, and optimization of dimensional accuracy of FDM-fabricated parts using definitive screening design and deep learning feedforward artificial neural network. *Adv Manuf* 9(1):115–129. <https://doi.org/10.1007/s40436-020-00336-9>
17. Hanon MM, Zsidai L, Ma Q (2021) Accuracy investigation of 3D printed PLA with various process parameters and different colors. *Mater Today Proc* 42:3089–3096. <https://doi.org/10.1016/j.matpr.2020.12.1246>
18. Alsoufi MS, Alhazmi MW, Suker DK, Alghamdi TA, Sabbagh RA, Felemban MA, Bazuhair FK (2019) Experimental characterization of the influence of nozzle temperature in FDM 3D printed pure PLA and advanced PLA+. *Am J Mech Eng* 7(2):45–60. <https://doi.org/10.12691/ajme-7-2-1>
19. Agarwal KM, Shubham P, Bhatia D, Sharma P, Vaid H, Vajpeyi R (2021) Analyzing the impact of print parameters on dimensional variation of ABS specimens printed using fused deposition modelling (FDM). *Sens Int* 3:100149. <https://doi.org/10.1016/j.sintl.2021.100149>
20. Robles GS, Delda RNM, Del Rosario RLB, Espino MT, Dizon JRC (2022) Dimensional accuracy of 3D-printed acrylonitrile butadiene styrene: effect of size, layer thickness, and infill density. *Key Eng Mater* 913:17–25. <https://doi.org/10.4028/p-nxviqm>
21. Bolat Ç, Ergene B (2022) An investigation on dimensional accuracy of 3D printed PLA, PET-G and ABS samples with different layer heights. *Çukurova Üniversitesi Mühendislik Fakültesi Dergisi* 37(2):449–458. <https://doi.org/10.21605/cukurovaumfd.1146401>
22. Suaidi SNSW, Azizul MA, Sulaiman S, Hao TY (2020) Effect of fused deposition modelling process parameters on the quality of ABS product. *J Ind Eng Innov* 2(1):9–9. <https://fazpublishing.com/jiei/index.php/jiei/article/view/43>
23. Mohanty A, Nag KS, Bagal DK, Barua A, Jeet S, Mahapatra SS, Cherkia H (2022) Parametric optimization of parameters affecting dimension precision of FDM printed part using hybrid Taguchi-MARCOS-nature inspired heuristic optimization technique. *Mater Today Proc* 50:893–903. <https://doi.org/10.1016/j.matpr.2021.06.216>

24. Akbaş OE, Hira O, Hervan SZ, Samankan S, Altinkaynak A (2019) Dimensional accuracy of FDM-printed polymer parts. *Rapid Prototyp J* 26(2):288–298. <https://doi.org/10.1108/rpj-04-2019-0115>
25. Zharylkassyn B, Perveen A, Talamona D (2020) Effect of process parameters and materials on the dimensional accuracy of FDM parts. *Mater Today Proc.* <https://doi.org/10.1016/j.matpr.2020.11.332>
26. Polak R, Sedlacek F, Raz K (2017) Determination of FDM printer settings with regard to geometrical accuracy. *DAAAM Proc* 0561–0566. <https://doi.org/10.2507/28th.daaam.proceedings.079>
27. Frunzaverde D, Cojocaru V, Ciubotariu C-R, Miclosina C-O, Ardeljan DD, Ignat EF, Marginean G (2022) The influence of the printing temperature and the filament color on the dimensional accuracy, tensile strength, and friction performance of FFF-printed PLA specimens. *Polymers* 14(10):1978. <https://doi.org/10.3390/polym14101978>
28. Botean AI (2018) Thermal expansion coefficient determination of polylactic acid using digital image correlation. *E3S Web of Conferences* 32, 01007. <https://doi.org/10.1051/e3sconf/20183201007>
29. Valerga AP, Batista M, Puyana R, Sambruno A, Wendt C, Marcos M (2017) Preliminary study of PLA wire colour effects on geometric characteristics of parts manufactured by FDM. *Procedia Manuf* 13:924–931. <https://doi.org/10.1016/j.promfg.2017.09.161>
30. Beniak J, Šooš L, Križan P, Matuš M, Ruprich V (2022) Resistance and strength of conductive PLA processed by FDM additive manufacturing. *Polymers* 14(4):678. <https://doi.org/10.3390/polym14040678>
31. Soares JB, Finamor J, Silva FP, Roldo L, Cândido LH (2018) Analysis of the influence of polylactic acid (PLA) colour on FDM 3D printing temperature and part finishing. *Rapid Prototyp J* 24(8):1305–1316. <https://doi.org/10.1108/rpj-09-2017-0177>
32. Vasudevarao B, Natarajan DP, Henderson M, Razdan A (2000) Sensitivity of RP surface finish to process parameter variation 251. *Repositorios.lib.utexas.edu.* <https://doi.org/10.26153/tsw/3045>
33. Nidagundi VB, Keshavamurthy R, Prakash CPS (2015) Studies on parametric optimization for fused deposition modelling process. *Mater Today Proc* 2(4–5):1691–1699. <https://doi.org/10.1016/j.matpr.2015.07.097>
34. Alafaghani A, Qattawi A, Alrawi B, Guzman A (2017) Experimental optimization of fused deposition modelling processing parameters: a design-for-manufacturing approach. *Procedia Manuf* 10:791–803. <https://doi.org/10.1016/j.promfg.2017.07.079>
35. Valerga A, Batista M, Salguero J, Girot F (2018) Influence of PLA filament conditions on characteristics of FDM parts. *Materials* 11(8):1322. <https://doi.org/10.3390/ma11081322>
36. Benwood C, Anstey A, Andrzejewski J, Misra M, Mohanty AK (2018) Improving the impact strength and heat resistance of 3D printed models: structure, property, and processing correlations during fused deposition modeling (FDM) of poly(lactic acid). *ACS Omega* 3(4):4400–4411. <https://doi.org/10.1021/acsomega.8b00129>
37. Kaveh M, Badrossamay M, Foroozmehr E, Hemasian Etefagh A (2015) Optimization of the printing parameters affecting dimensional accuracy and internal cavity for HIPS material used in fused deposition modeling processes. *J Mater Process Technol* 226:280–286. <https://doi.org/10.1016/j.jmatprotec.2015.07.012>

Publisher's Note

Springer Nature remains neutral with regard to jurisdictional claims in published maps and institutional affiliations.

Submit your manuscript to a SpringerOpen[®] journal and benefit from:

- Convenient online submission
- Rigorous peer review
- Open access: articles freely available online
- High visibility within the field
- Retaining the copyright to your article

Submit your next manuscript at ► [springeropen.com](https://www.springeropen.com)
